Equilibrium polymerization in the Stockmayer fluid as a model of supermolecular self-organization

Kevin Van Workum* and Jack F. Douglas†
Polymers Division, National Institute of Standards and Technology, Gaithersburg, Maryland 20899, USA
(Received 5 August 2004; published 2 March 2005)

A diverse range of molecular self-organization processes arises from a competition between directional and isotropic van der Waals intermolecular interactions. We conduct Monte Carlo simulations of the Stockmayer fluid (SF) with a large dipolar interaction as a minimal self-organization model and focus on basic thermodynamic properties that are needed to characterize the polymerization transition that occurs in this fluid. In particular, we determine the polymerization transition lines from the maximum in the specific heat, C_v, and the inflection point in the extent of polymerization, Φ. We also characterize the geometry (radius of gyration R_g, chain length L, chain topology) of the clusters that form in this associating fluid as a function of temperature, T, and concentration, ρ. The pressure, P, and the second virial coefficient, B_2, were determined, since these properties contain essential information about the strength of the isotropic (van der Waals) interactions. Our simulations indicate that the locations of the polymerization lines are quantitatively consistent with a model of equilibrium polymerization with the enthalpy of polymerization ("sticking energy") fixed by the minimum in the intermolecular potential. The polymerization transition in the SF is accompanied by a topological transition from predominantly linear to ring polymers upon cooling that is driven by the minimization of the dipolar energy of the clusters. We also find that the basic interaction parameters describing polymerization and phase separation in the SF can be estimated based on the existing theory of equilibrium polymerization, but the theory must be refined to account for ring formation in order to accurately describe the configurational properties of this model self-organizing fluid.

DOI: 10.1103/PhysRevE.71.031502 PACS number(s): 61.20.−p, 64.60.Cn, 05.65.+b, 81.16.Fg

I. INTRODUCTION

The increasing demand to manufacture structures at the nanoscale has made it necessary to pursue new fabrication strategies. Many researchers have taken inspiration from biological systems that exploit supermolecular self-assembly to form complex hierarchical structures of specific function and structure and have developed synthetic molecular systems exhibiting this kind of self-organization [1–5]. Others have harnessed biological systems such as viruses to perform this function [6]. This approach is highly attractive for the fabrication of large-scale devices from nanoscale or molecular components, but the *control* of this type of process remains largely a dream. Progress in this area requires an understanding of the basic principles that underlie the molecular self-assembly process [7–10]. Precise control of synthesis is required [1–3], along with theoretical principles that can predict what structures form and the conditions under which they are stable.

In our view, a major shortcoming in the control of molecular self-organization for fabrication is the lack of understanding of the interplay between molecular potential interactions (which are often highly directional rather than "unspecific" as in van der Waals interactions) and the thermodynamics governing these self-organization transitions. We also need to know the different kinds of thermodynamic transitions that occur (and their associated phase boundaries), the physical interaction parameters that govern them, and the changing molecular dynamics that accompany these transitions. It is also important to understand how these self-organization transitions couple to phase separation and other transitions (e.g., liquid crystalline ordering) to create new hybrid or hierarchical transitions [11–15]. Advances in this field have ramifications for understanding biological processes, as well as providing a versatile tool in developing new materials, devices, and pharmaceuticals [7].

Our approach to this fundamental problem is to isolate a minimal physical model of molecular self-organization and to intensively investigate this model through a combination of Monte Carlo and analytical modeling (molecular dynamics simulations are planned for a later stage). We selected the classical Stockmayer fluid (SF) [16] for this purpose since it involves a minimal description of the interplay of directional (dipolar) and isotropic (Lennard-Jones van der Waals) interactions that have been suggested to fundamentally underlie many supermolecular self-organization processes [17–19]. This choice is also motivated by the existence of *exact* analytic results for the second [20] and third virial coefficients [20–23] of this model and by extensive previous MC simulations [24,25] of the critical properties (critical temperature, critical composition, compressibility factor, etc.) relating to phase separation in this model.

The SF model is also known through many studies to exhibit supermolecular organization into dynamic polymer chains through a head-to-tail alignment of the dipolar fluid particles [26,27]. There have been many recent articles attempting to understand the coupling between phase separation and this molecular self-organization process [28–30], but many aspects about this model remain largely unresolved because of the general difficulty of performing simulations on associating fluids and the corresponding difficulty in theo-

*Electronic address: kevin.vanworkum@nist.gov
†Electronic address: jack.douglas@nist.gov

retically describing these intrinsically heterogeneous fluids [29]. In the end, our choice of the SF as a model of molecular self-organization was dictated by the limitations of existing computational resources. Simulation of equilibrium properties of this type of self-organizing system must include a minimal description of the essential characteristic of this process, a competition between directional and isotropic interactions.

Although the SF model is rather idealized, it does have some interest as a model of real self-organization processes of practical interest. It is a reasonable model of the stringlike self-organization of magnetic nanoparticles [26,27] and the self-organization of molecular wires [18]. These classes of materials have a growing number of technological applications [17,18,29]. Certain bacteria [31], and presumably other biological systems, exploit the self-organization of iron oxides and iron sulfide particles which they synthesize for directional navigation, and these ferrofluids are quite reasonably described by the SF. Recently, it has been possible to synthesize a wide range of magnetic nanoparticle systems exhibiting chain formation [32,33] and directly observe this process.

The SF also seems to be a promising model for the self-assembly of synthetic peptides and other biological macromolecules into thermally reversible gels comprised of self-organized fibers of molecular chains of these folded peptides [34]. The formation of fiberlike structures also occurs in amyloid proteins found in association with Alzheimer's disease [34]. Moreover, strong dipolar interactions have been indicated to be essential in microtubule self-assembly [35], a part of the essential cell machinery for many complex organisms responsible for driving chromosome separation and facilitating molecular transport within the cell. As a final point, we mention that the SF provides a rather idealized model of water, which is characterized by having a rather large dipole moment. Many of the unique properties of water derive from its associating characteristics [35]. The natural extension of the SF model to include quadrupole interactions [107] would make the model an even closer mimic of this complex fluid.

There have been numerous previous studies of the SF. The early work in the 1940s was concerned with the influence of dipolar interactions on the thermodynamic properties of gases [20,20–23,36–38] and the deviation from the corresponding states description of the critical properties of dipolar fluids [39]. The prevalence of dipolar fluids to cluster at equilibrium and the impact of this clustering on the properties of these fluids were appreciated from the beginning of these investigations [36,37]. The direct observation of chain formation in ferrofluids of magnetic particles dispersed in various organic solvents alerted researchers to the extent to which these simple systems can self-organize into complex structures and the sensitivity of these fluids to external magnetic fields [40,41].

The difficulties that this clustering created for conventional mean-field liquid-state theories were slow to develop, but simulation soon pointed to serious failures of models that have proven their value for homogeneous fluids [24]. The intense activity in simulating the SF and related idealized models of dipolar fluids (soft-sphere-dipole fluids [42], dipolar hard-sphere model [43,44], spherocylinder with dipolar interactions [45], etc.) has come as a consequence of the realization that these fluids can exhibit thermodynamic and critical properties completely unlike those of "simple" fluids [46,47]. A substantial impetus to studying the SF arose in particular because of two remarkable recent findings: (i) the observation of ferroelectric behavior in simulations of dipole soft-sphere fluid in the liquid state in association with chain formation [42], and (ii) the apparent *disappearance* of the critical point for phase separation when the magnitude of the dipolar interaction became critically large relative to the magnitude of the van der Waals interaction energy [24,25,45]. These works have set off an avalanche of activity relating to the SF and related dipolar fluid models.

Since the polymerization of the dipolar particles is clearly at the origin of many of the peculiar properties of dipolar fluids, there have been many recent studies attempting to characterize this transition as a variety of "equilibrium polymerization" [28,30,48,49]. Teixeira *et al.* [29] give a good review of the successes and limitations of these efforts. This previous work clearly indicates that associating dipolar fluids are very interesting, but computational methods of sufficient power to simulate or to analytically model these fluids do not currently allow for a resolution of the many outstanding questions.

The present work is an extension of previous efforts, but our work has a different focus. Our first concern is to implement an efficient numerical sampling method for simulating the SF at low density and to determine the location of the polymerization transition line. We determine these transition lines as an experimentalist would approach the problem and strive to avoid any bias regarding the theoretical interpretation of this transition, since a reliable theory does not clearly exist. Recent theoretical computations by Dudowicz *et al.* [11,12,30] and others [28,48,49] suggest models that might apply, but we do not presume the correctness of these models before they are validated by reliable simulations.

The exact relation between the transition curves governing the chain formation process and the molecular interaction parameters is a key concern in our investigation. Notably the polymerization transition lines have never been determined before in the SF. We illustrate the utility of the polymerization transition determination for the quantification of the properties of the self-organizing fluid by showing that a universal description of the chain length as a function of temperature and concentration can be obtained by introducing a reduced temperature scale based on the concentration-dependent location of the polymerization transition. Equation of state ideas are evidently a powerful tool describing molecular self-organization as well as describing the critical properties of simple fluids.

In the course of our characterization of the density, ρ, dependence of the chain length, L, we found that this property scales in proportion to ρ rather than $\rho^{1/2}$, as in analytic models suggested to describe this type of polymerization [11,12,50]. The exponent describing the T dependence of L is similarly almost doubled from the "expected" value. Unfortunately, this indicates that all the proposed models of equilibrium polymerization in the SF are inadequate for a completely quantitative description of the SF. Further investigation revealed that the SF with a strong dipolar inter-

action exhibits topological transitions between linear and ring polymers upon cooling. The character of this transition appears *qualitatively inconsistent* with the transition between linear and branched chains predicted by Tlutsy and Safron [51], however (see Sec. III C).

Ring formation occurs at low temperature simply because this minimizes the energy of the dipolar chain [52]. Since this topological transition between chain and ring polymers was not initially anticipated and this phenomenom is not incorporated in current models of equilibrium polymerization in this fluid, we examined the configurational properties of the chains in greater detail. We observed a bimodal distribution of the radius of gyration of the polymers corresponding to coexisting linear and ring structures and found that the R_g mass scaling exponent was consistent with polymer chains with excluded volume interactions and some degree of stiffness arising from the dipolar interactions. We also note that the mass scaling exponent describing the swelling of the polymer chains is consistent with an equilibrium polymerization formulation of the *XY* model in which directed polymer loops geometrically form in association with the transition [53–55].

Finally, we examined the pressure and second virial coefficient of the SF since these and related properties provide essential experimental information regarding the magnitude of both the van der Waals and the directional (dipolar) interactions driving the molecular self-organization. We were able to calculate the Boyle (or "theta") point exactly for the SF model for arbitrary dipolar and van der Waals interactions, and we validated our simulations against exact analytic calculations of the second virial coefficient [16,20] as a function of T and the dipolar interaction. These results show that a reliable estimate of the van der Waals interactions can be extracted from measurements of the pressure (or compressibility) at low concentrations, despite the slow variation of the pressure at higher ρ arising from the polymerization process.

In summary, we have simulated the SF model over a wide range of T and ρ using an efficient computational method, and we have determined the essential thermodynamic parameters that govern the self-organization of the particles into chain structures by mapping out the polymerization transition line as a function of T and ρ. We show that the van der Waals interaction parameter governing phase separation can still be determined in the conventional way from the second virial coefficient of P.

II. SIMULATIONS

We perform canonical ensemble Monte Carlo (MC) simulations of the Stockmayer fluid in cubic simulation boxes with periodic boundary conditions. In the Stockmayer model [16], two particles interact via the Lennard-Jones (LJ) potential with an additional point dipole at each particle center. The interactions between particle pairs are truncated at half the box length. Using this boundary condition, our evaluations of the second virial coefficient (Fig. 15) agree with the exact analytical solution and with sample runs using the full Ewald summation method. The use of this cutoff procedure should be reevaluated for simulations at higher densities than reported here. The LJ contribution to the total energy is given by

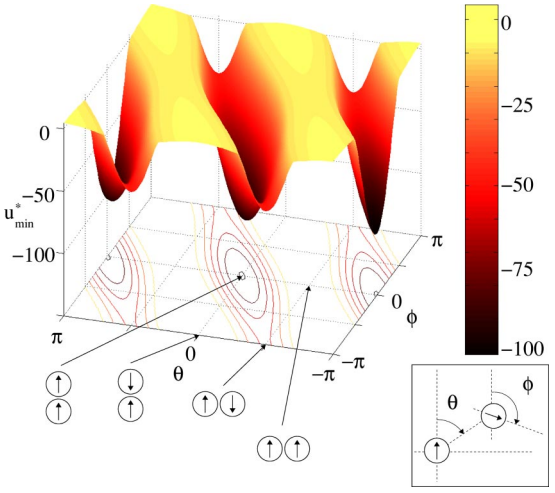

FIG. 1. (Color online) $u^*_{\min}=u_{\min}(\theta,\phi)/\varepsilon$ for the Stockmayer model with $\mu^{*2}=36$.

$$u_{LJ}=4\varepsilon\left[\left(\frac{\sigma}{r_{ij}}\right)^{12}-\left(\frac{\sigma}{r_{ij}}\right)^{6}\right], \tag{1}$$

where r_{ij} is the distance between particles i and j, ε is the magnitude of the potential minimum, and σ is the separation at which the energy vanishes. The simulation boxes contain 256 particles and have edges ranging in length from 23.4σ to 64.5σ so that the density range is $0.003\,18\leqslant\rho/\rho_{c,LJ}\leqslant 0.0637$, where $\rho_{c,LJ}=0.316\sigma^{-3}$ is the critical density of the LJ fluid [56]. All densities reported in this paper are normalized by $\rho_{c,LJ}$ and all temperatures are normalized by $T_{c,LJ}=1.31\varepsilon/k_B$, the LJ critical temperature [56]. This normalization procedure is used to facilitate comparison with the lattice models of equilibrium polymerization described later in the text.

The dipolar contribution to the energy is given by

$$u_{\text{dipole}}=\frac{\vec{\mu}_i\cdot\vec{\mu}_j}{r_{ij}^3}-3\frac{(\vec{\mu}_i\cdot\vec{r}_{ij})(\vec{\mu}_j\cdot\vec{r}_{ij})}{r_{ij}^5}, \tag{2}$$

where $\vec{\mu}_i$ is the dipole moment of particle i and $\vec{r}_{ij}=\vec{r}_j-\vec{r}_i$ is the separation vector between particles i and j. In the literature, it is conventional to define a dimensionless dipole moment, $\mu^*=\mu/\sqrt{\varepsilon\sigma^3}$. The total energy is given by $u=u_{LJ}+u_{\text{dipole}}$. For all simulations reported here, the magnitude of the dipole strength is given by $\mu^{*2}=36$ unless otherwise stated. With this choice of dipole strength, the dipolar contribution to the minimum in the potential is roughly 100 times that of the LJ contribution.

The anisotropy in the potential is illustrated in Fig. 1, which shows the minimum of the Stockmayer potential as a function of fixed relative orientations of the two particles for $\mu^*=6$. The deep minimum corresponds to a head-to-tail alignment of the dipoles and a particle separation $r=0.8295\sigma$. The potential at this minimum is $u_{\min}=-100.7\varepsilon$

for this choice of μ^*. More generally, the magnitude of this potential minimum, ε_{μ^*}, can be described exactly by

$$\varepsilon_{\mu^*} = 4\varepsilon\left[\frac{\mu^{*2}}{2}\left(\frac{\sigma}{r_{\min}}\right)^3 + \left(\frac{\sigma}{r_{\min}}\right)^6 - \left(\frac{\sigma}{r_{\min}}\right)^{12}\right], \quad (3)$$

$$\frac{r_{\min}}{\sigma} = \left[\frac{1}{3\mu^{*2}}\left(2^{2/3}\lambda - 4 + \frac{2^{1/3}8}{\lambda}\right)\right]^{1/3}, \quad (4)$$

$$\lambda = \left[27\mu^{*4} + 3\mu^{*2}\sqrt{3(27\mu^{*4} - 32)} - 16\right]^{1/3}, \quad (5)$$

where ε is the magnitude of the potential minimum for $\mu^* = 0$ (the LJ minimum). It can be shown that ε_{μ^*} has a nonanalytic dependence on μ^* and has the limiting asymptotic behavior

$$\lim_{\mu^* \to \infty} \varepsilon_{\mu^*}/\varepsilon \sim 3\mu^{*8/3}/4. \quad (6)$$

We can obtain a good approximation to ε_{μ^*} by simply adding an additional nonanalytic term and a constant and fixing their values by demanding that the exact value of ε_{μ^*} be recovered for $\mu^* = 2$ ($\varepsilon_{\mu^*} = 8\varepsilon$) and $\mu^* = 0$ ($\varepsilon_{\mu^*} = \varepsilon$),

$$\varepsilon_{\mu^*}/\varepsilon \approx 1 + 0.888\,07\mu^{*4/3} + 3\mu^{*8/3}/4. \quad (7)$$

This expression agrees with the exact result from Eq. (3) to within an accuracy of 2% for arbitrary positive μ^*, apart from the range (0.08,1.4) over which a crossover from LJ dominated to dipole-dominated potential behavior occurs [25]. Equation (7) provides a general estimate of the "sticking energy" in our comparisons with the equilibrium polymerization model below and is a basic input into this type of analytic model. The nonanalytic dependence of ε_{μ^*} derives from the soft nature of the potential core interaction in the LJ fluid, and we contrast Eq. (7) with the corresponding result for hard spheres with a point dipolar interaction where $\varepsilon_{\mu^*,HS}/\varepsilon = 2\mu^{*2}$. The hard-sphere expression for $\varepsilon_{\mu^*,HS}$ is a reasonable approximation for the SF provided that μ^* is not too large or too small (i.e., to within 2% for $1.61 < \mu^* < 2.52$) and is exact for $\mu^* = 2$.

The minimum energy configuration of a finite, unbranched polymer is a ring, but entropy effects favor open chain configurations at high temperatures [52]. The stiffness of the chain is related to the shape of the energy basin in Fig. 1. At intermediate T, there is a coexistence of rings and chains. Because branching "Y-like" junctions have a lower energy than free ends, connected networks are likely to also form at lower temperatures as transient structures [51,57]. Thus, the particles associate to form linear chains, rings, and hybrid branched structures ("clusters") in dynamic equilibrium [27,51,57]. Ring-chain equilibrium has also been observed in models of reversibly associating polymer solutions [58].

At gas phase densities, the simulation of strongly associating systems can present challenges for traditional simulation techniques. The strong binding energies between associated particles and large distances between nonassociated particles can make sampling of important regions of configuration space difficult [59]. The time required for particles to undergo an association-disassociation transition can be very long compared to typical molecular-dynamics simulation times. There are MC algorithms that can overcome these difficulties, however.

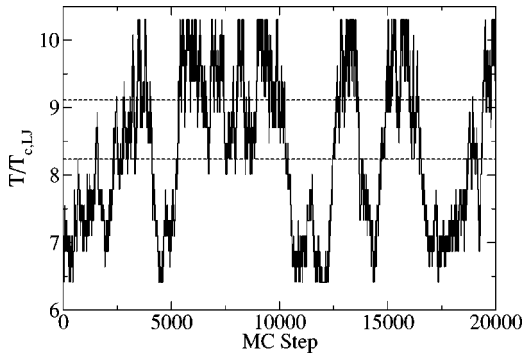

FIG. 2. Temperature versus MC step for a representative replica. The T_Φ and T_p (discussed later) are shown as dotted lines for reference.

In this work, we use the aggregate bias Monte Carlo algorithm [60] to improve the sampling of relevant regions of configuration space and enhance the formation of clusters. This method allows for the simulation of chain, ring, and branched forming molecules. At the heart of this algorithm is an intrabox swap move that is targeted at sampling the formation or destruction of clusters. We also implement the simple translational and rotational moves to explore nearby regions of phase space.

When implementing the simulation of strongly associating systems, proper statistical sampling can be difficult at low temperatures where configurations may become trapped in local energy minima. Traditional MC algorithms may not be capable of sampling the relevant regions of phase space within a reasonable amount of time. Parallel-tempering [61,62] is a useful technique that has been used in the study of thermodynamic transitions and can be efficiently applied to the simulation of associating fluids.

In this study, each simulation is performed within the parallel-tempering framework. This method employs a set of canonical ensemble simulation boxes running in parallel at different temperatures, but with the same number of molecules and the same density. Boxes are arranged in order of increasing temperature, and periodically, random adjacent pairs of boxes are chosen and a swap move is attempted. In the present study, 18 boxes were used at each density and adjacent boxes differed in temperature by $\Delta T/T_{c,LJ} = 0.229$. This allows adequate swapping while still maintaining a relevant T range within the constraint of available computational resources. In a successful swap move, the atoms in one box are exchanged with those in the other box. Effectively, configurations take a one-dimensional random walk in T space. Swap moves are accepted with a probability given by

$$p_{a \leftrightarrow b} = \min[1, \exp\{\Delta U \Delta\beta\}], \quad (8)$$

where $\Delta U = U_b - U_a$ is the potential energy difference of the systems, and $\Delta\beta = 1/(k_B T_b) - 1/(k_B T_a)$.

Figure 2 shows the temperature of an example configura-

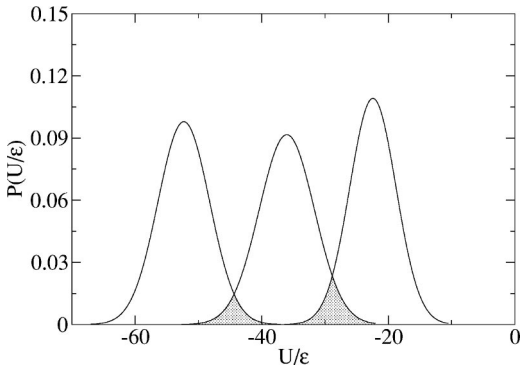

FIG. 3. Energy probability distribution functions for $T/T_{c,LJ}=6.64,6.87,7.10$ at $\rho/\rho_{c,LJ}=0.00318$. At this density, $T_p/T_{c,LJ}=6.72$ and $T_\Phi/T_{c,LJ}=6.87$.

tion versus MC step during a simulation run as it steps from box to box. It is evident that configurations are sampling the full temperature range within the parallel-tempering algorithm. This allows lower T simulations to benefit from the faster motions available at higher T, thereby leading to faster equilibration. In addition, the swapping of configurations reduces the time spent in local minima and allows the system to explore phase space more effectively.

To ensure that configuration swapping moves are accepted at an efficient rate, adjacent boxes must be close enough together in T space to allow their energy histograms to sufficiently overlap. Figure 3 shows the adequate overlap of the energy histograms of the lowest density box at a temperature ($T/T_{c,LJ}=6.87$) near its polymerization temperature ($T_p/T_{c,LJ}=6.72$) and that of two adjacent boxes ($T/T_{c,LJ}=6.64$ and 7.10). At this density, the energy histograms are at their sharpest and at all other densities the overlap of adjacent energy histograms increases at the polymerization transition. Figure 3 thus shows a worst case scenario for simulations in this study. Each system was equilibrated for a minimum of 10^7 MC steps and thermodynamic averages were computed using a minimum of 10^7 MC steps, where an MC step consists of an attempt to translate and rotate every particle in the box. Parallel-tempering swaps were attempted every 25 MC steps.

III. RESULTS

The present paper specifically avoids an investigation of the critical properties and analytic modeling of the impact of the polymerization process on the critical properties of the SF since these properties have been a topic of intensive study in previous work [24,25,28–30]. We have chosen μ^* to equal a value larger than the critical value $\mu^*\approx 5$ for which phase separation has been claimed not to exist in the SF [24,25]. We saw no evidence for conventional phase separation in our computations in the parameter regime we investigated, so that we feel we have successfully avoided questions relating to the phase separation of the SF. We note, however, that the former MC simulations of the SF were based only on simple Gibbs MC sampling methods, and the equilibration times were short by current standards. Thus, the characterization of the critical behavior of the SF should also be revisited with the computational methods described in the present paper, or by alternative methods (e.g., density of states [63]) that have recently proved their value in simulating supercooled liquids and other kinetically sluggish thermodynamic systems [64].

A. Polymerization transition lines

The polymerization transition line is basic to understanding the thermodynamic properties of the type of particle self-organization observed in the SF. This type of transition line is comparable in importance to phase boundaries in ordinary phase separation because they contain basic information about thermodynamic interactions responsible for the transition. Such transition lines are well known in micelle forming liquids [65–67], but also occur much more broadly in systems undergoing living polymerization [e.g., poly(α-methyl styrene) in solution in the presence of a chemical initiator [68]], thermally activated polymerization (actin, sulfur) [69,70], clustering in polymer nanocomposites [71], and thermal reversible gelation of polymers [72–77], colloids [78–80], and low molecular mass organogels [17–19]. The location of the polymerization transition temperature as a function of concentration ("polymerization line") has never before been determined in the SF and we first focus on this quantity.

The most common way to define the polymerization transition line is through the constant volume heat capacity, C_v [81–83]. Normally, the transition between a particle-dispersed state and a state in which the particles are organized into specific structures is accompanied by a maximum in the heat capacity. The T where this maximum occurs is taken as the "polymerization" or "clustering" transition temperature, T_p. We thus consider C_v for the SF as a function of T and ρ.

Before calculating T_p as a function of ρ, we note that there is another conventional criterion determining the polymerization transition line that is utilized by experimentalists because of the difficulty in measuring C_v [69,81,82]. The polymerization transition line is also defined through the extent of polymerization, Φ,

$$\Phi = N_p/N, \tag{9}$$

where N_p is the number of associated particles and N is the total number of particles. Two particles are considered to be in a cluster if the separation distance is less than $r_a=1.5\sigma$, i.e., approximately where the interaction energy is at least 20% of the potential minimum. The location of the transition lines is expected to be insensitive to small changes in the definition of r_a. The transition T is defined as the inflection point in Φ as a function of T, and we denote this quantity in the present paper as T_Φ. The property Φ is an "order parameter" for the polymerization model describing the extent to which the polymerization transition has gone to completion [13,81–83].

The constant volume heat capacity, C_v, is calculated from the fluctuations of the potential energy at each temperature and density. The heat capacity is given by

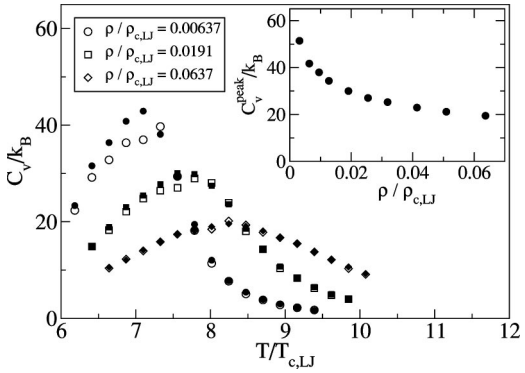

FIG. 4. Constant volume heat capacity, C_v, versus T. Filled symbols are from derivatives of the potential energy and open symbols are from fluctuations of the potential energy. Inset shows peak values of C_v versus ρ. Estimated uncertainties according to the method of Ref. [84] are on the order of the size of the symbols.

$$C_v = \frac{1}{Nk_BT^2}[\langle U^2\rangle - \langle U\rangle^2]. \tag{10}$$

The constant volume heat capacity can also be calculated by directly differentiating the potential energy with respect to T,

$$C_v = \frac{1}{N}\frac{\partial U}{\partial T}. \tag{11}$$

Figure 4 shows the heat capacity as a function of temperature for three densities calculated using Eqs. (10) and (11). The quantitative agreement between the two methods of computing C_v is encouraging. We observe that the peak in the heat capacity occurs at lower T for lower densities, as predicted by the theory of equilibrium polymerization [83]. A similar pattern of behavior was observed recently for model nanoparticles clustering in a polymer melt by molecular dynamics simulations [71]. As discussed by Starr *et al.* [71], this trend is quite distinct from what we would expect if the "clustering" were due to phase separation. At higher densities, the peak becomes broader. The inset of Fig. 4 indicates that the magnitude of C_v is increasing with decreasing ρ. This is an indication that a vapor to liquid phase transition is not occurring. The T at which the peak occurs at each density is termed the *polymerization temperature* and is denoted by T_p.

Figure 5(a) plots the extent of polymerization, Φ, versus temperature for a number of densities. The transition temperature T_Φ is defined as the inflection point T in the Φ versus T curve. At low temperatures, nearly all the particles can be incorporated into individual clusters, while at high temperatures most particles exist as free monomers. It is stressed that the monomer units are in *thermodynamic equilibrium* with the clusters. The clusters grow or diminish in size as particles (or other clusters) join or leave the clusters. Similarly to C_v, the transition becomes sharper and grows at lower densities. Figure 5(b) shows Φ as a function of ρ at constant T. The polymerization transition can proceed at constant T by increasing the density. From Fig. 5(b) we see that the transition is sharper at lower T.

It has often been assumed that the polymerization transition, as defined through C_v, is equivalent to the polymerization transition temperature determined from the inflection point of Φ [81,82]. This expectation is apparently based on the exact coincidence of these transition points in the successful mean-field theory of living polymerization; this relation holds regardless of the initiator concentration [13,83]. Recent work of Dudowicz *et al.* [30] has indicated that these transition temperatures are *not* the same in more general models of equilibrium polymerization, however. In particular, the analytic theory of equilibrium polymerization without the constraint of an initiator (termed the freely associating or FA model [30]) [50] has been suggested to describe the equilibrium polymerization in the SF [28,30,48,49]. In this model, every particle can freely associate with any other particle without restriction, and T_Φ is found to occur substantially above T_p [83].

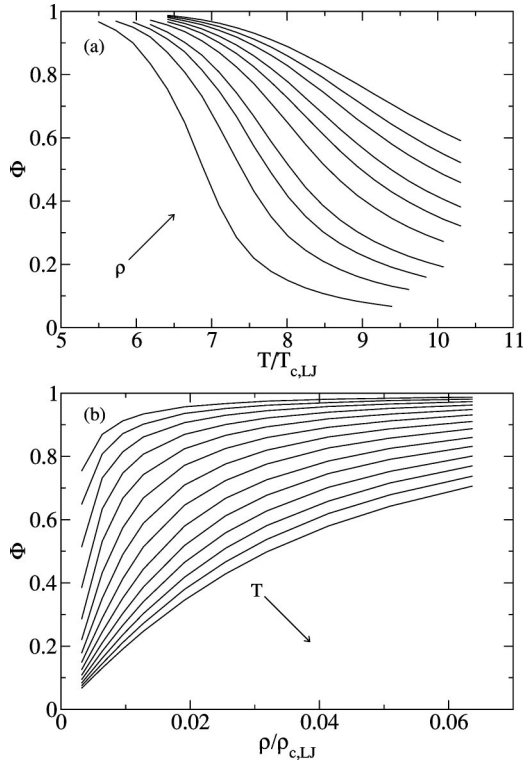

FIG. 5. Extent of polymerization versus temperature (a) and versus density (b). Arrows denote increasing ρ and T, respectively. The estimated uncertainties [84] for Φ are less than 1%.

In Fig. 6, we show the values of T_p and T_Φ that we determined from our simulations (see Figs. 4 and 5). We see that T_Φ is indeed larger than T_p over the density range investigated and that these curves tend to come together at low density. Comparison to Fig. 4b of Ref. [83] demonstrates good qualitative agreement between the shapes of the transition lines predicted by the FA model and the SF.

Unfortunately, there is no closed exact analytic formula describing the polymerization transition line in the FA model [83], but there is a simple estimate of the polymerization transition line in the related model of "living polymerization" in the limit of vanishing initiator [13,83]. In this model, the polymerization transition line (T_p) is described by the so-called Dainton-Ivin equation [85],

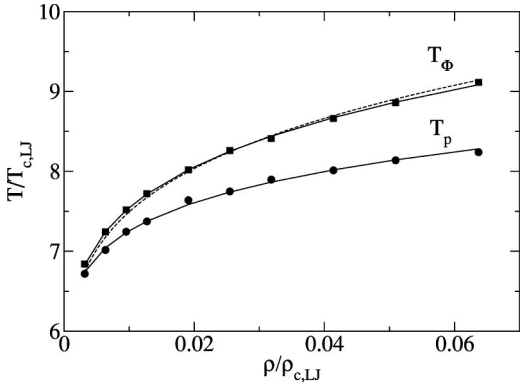

FIG. 6. Transition temperatures versus density. Lines are fits to the DI equation.

$$T_p(\mathrm{DI}) = \frac{\Delta h_p}{\Delta s_p + k_B \ln \rho}, \tag{12}$$

where Δh_p and Δs_p are the changes in the enthalpy and entropy for the polymerization association (reaction) at a given concentration. Equivalently, Eq. (12) defines a "critical polymerization concentration," ρ_c having an Arrhenius form,

$$\rho_c = A \exp(\Delta h_p / k_B T), \tag{13}$$

where $A = \exp(-\Delta s_p / k_B)$. Equation (12) indicates a monotonic increase in T_p with ρ and is widely used to describe clustering transitions in equilibrium polymerization (living polymerization [81,82] and thermally activated polymerization [17–19,74]), as well as gelation, micellation [65,66], and other varieties of molecular self-organization at equilibrium. This Arrhenius form is often found to fit clustering transition data very well as a matter of phenomenology. The generality of Eqs. (12) and (13) in describing a wide range of self-organization processes other than the polymerization of linear chains supports the contention of universality in the thermodynamics of associating fluids suggested by Dudowicz *et al.* [11,12,83].

Dudowicz *et al.* [13] find that Eqs. (12) and (13) also describe the T_p and T_Φ transition curves of the FA model of equilibrium polymerization, but the interpretation of the model energetic parameters $(\Delta h_p, \Delta s_p)$ are not exactly the same as in the Dainton and Ivin model [85]. The problem is that the values of Δh_p and Δs_p can be "renormalized" in the fit to the DI equation from their exact values in the FA model.

The analytic theory of Dudowicz *et al.* [13] predicts that the transition temperature T_Φ remains close to the Dainton-Ivin transition curve and comparison of the simulation data to the DI curve should yield the most reasonable energetic parameters for the SF fluid. In Fig. 6, the "sticking" energy, Δh_p, is fixed in this expression to equal the potential energy minimum (contact energy) for SF particles in a head-to-tail arrangement, i.e., $\Delta h_p = -100.7\varepsilon$. A previous paper comparing the phase behavior of the SF to the FA model estimated $\Delta s_p / k_B$ to be roughly in the range -5 to -10, depending on the extent of chain stiffness, and similar order-of-magnitude estimates of Δs_p were noted years ago by Rowlinson for real dipolar gases [20]. The dashed line in Fig. 6 shows the DI equation with Δh_p *fixed* by the contact energy of the molecular potential and $\Delta s_p / k_B$ fitted to the value -4.5. A better fit (solid line) of the DI equation to the T_Φ data is obtained by letting both Δh_p and Δs_p vary. This procedure yields $\Delta h_p = -108\varepsilon$ and $\Delta s_p / k_B = -5.17$. The agreement with the expectations of the equilibrium polymerization model is highly encouraging. The former best estimate of $\Delta s_p / k_B$ for the SF, based on a study of phase separation in this model for lower μ^* and an assumption that the chains were stiff (flexible), is $\Delta s_p / k_B = -5.9(-8.5)$.

The renormalization of the energetic parameters governing the T_p transition line is predicted to be more appreciable than for the T_Φ transition line [13]. A fitting of the DI equation to the FA-model prediction of T_p [13,86] indicates that the apparent value of Δh_p obtained from this fit is related to the true value of Δh_p by the approximation (assumption of flexible chains)

$$\Delta h_p^{\mathrm{app}} / \Delta h_p^{\mathrm{tr}} = 1.014 + 1.602 \exp(0.327\ \Delta s_p / k_B), \tag{14}$$

where the maximum deviation in the approximation is less than 1.4 % for $-28.7 < \Delta s_p / k_B < -4.6$. For $\Delta s_p / k_B = -4.5$ and $\Delta h_p^{\mathrm{tr}} = -100.7\varepsilon$, this relation predicts that $\Delta h_p^{\mathrm{app}}$ obtained from a fit to T_p should equal -132ε. [Notably, this effective value of Δh_p is not a correct estimate of the enthalpy of association, but rather an apparent value obtained by fitting T_p data to Eq. (12).] A fit of the DI equation to the T_p data in Fig. 6 (solid line) yields $\Delta h_p^{\mathrm{app}} = -142\varepsilon$, which is in reasonable agreement with Eq. (14). This finding provides us with further encouragement that an equilibrium polymerization model can provide a quantitative description of the polymerization process in a molecular fluid.

One of the shortcomings of our current description of self-organization in the SF is the uncertainty in the estimation of Δs_p. This is a basic problem in describing equilibrium self-organization processes that has received rather little serious attention. Economou and Donohue [87] have provided the basis for attacking this problem by showing the formal equivalence between chemical association theory and the classic liquid state theory of associating fluids developed by Wertheim [88]. This correspondence provides a direct formal route to calculating Δs_p through liquid state correlation functions, although the approach has not yet been implemented. A fully predictive theory of equilibrium polymerization in terms of microscopic potential parameters requires the computation of Δs_p by such a method.

B. Average degree of polymerization

The next most basic property of a fluid undergoing equilibrium polymerization is the average degree of chain polymerization, L. This quantity is defined by [13,83]

$$L = \frac{\sum_{i=1}^{N} i N_i}{\sum_{i=1}^{N} N_i}, \tag{15}$$

where i is the number of particles in a given chain and N_i is the number of chains of length i. In Fig. 7, we show L as a

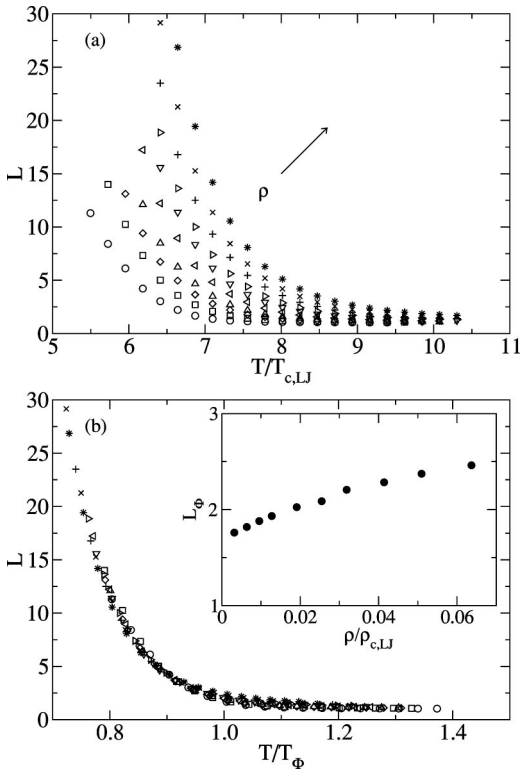

FIG. 7. Chain length of polymer. Average chain length versus temperature (a). Average chain length versus temperature normalized by T_Φ (b). The inset of (b) shows the average chain length at $T=T_\Phi$.

function of T for a range of T, and we find a family of curves describing the general increase of L upon cooling. At higher densities, the increase in $L(T)$ occurs faster as T is lowered, reflecting the ρ dependence of the polymerization transition. The curves in Fig. 7 notably have a similar shape, and it is natural to seek a reduced variable description.

Our discussion above indicates that, contrary to the opinions expressed in former work, the transition temperature T_Φ has a more fundamental significance as a definition of the transition point than the transition curve defined through C_v, regardless of the detailed nature of the association process. We thus define a reduced temperature T/T_Φ and examine the extent to which the transition curves shown in Fig. 7 reduce to a single master curve. The result of this data reduction is shown in Fig. 7(b). This definition of reduced temperature collapses the L data to a nearly universal function. An important characteristic of equilibrium polymerization is the near constancy [13] of L at the transition temperature T_Φ; $L_\Phi \equiv L(T_\Phi) \approx 2 \pm 0.5$ and estimates of L_Φ are shown in the inset to Fig. 7(b). Note that L_Φ is relatively small because of the large weight given to monomers in the determination of this average. The chains are actually highly polydisperse and this aspect of the SF has been investigated in previous work [28,48,49]. The near constancy of L_Φ can be understood from the FA equilibrium polymerization model where also $L_\Phi \approx 1.5$ and $L(T=T_p) \approx 3$, independent of ρ [86].

The dependence of the L on the ρ is shown in Fig. 8. At the lowest T, the degree of polymerization is nearly linear with respect to ρ. However, at higher T the linearity begins at

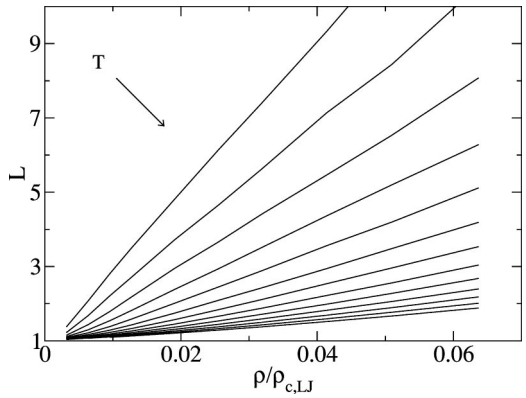

FIG. 8. Average degree of polymerization versus density. The arrow indicates the direction of increasing temperature. The estimated uncertainties [84] in L are less than 0.5% and are not included for clarity.

higher densities. The linear regions generally coincide with the relatively flat regions in the pressure versus density curves (see Sec. III D). The concentration dependence of L reflects the ρ dependence of Φ shown in Fig. 5. In the limit of vanishing concentration, we must have $L=1$, but L linearly increases beyond some T-dependent concentration, ρ_c, where polymerization initiates. Thus, we describe $L(\rho)$ by

$$L = 1 + \alpha(T)(\rho - \rho_c)\rho > \rho_c. \tag{16}$$

We note that more accurate determinations of the "critical polymerization concentration," ρ_c, can be obtained from Eq. (13) rather than Eq. (16) due to the uncertainty involved in determining the intercepts in Fig. 8.

Our examination of L as a function of ρ gives us our first hint that the simple FA model of equilibrium polymerization provides an overly simplified quantitative description of equilibrium polymerization in the SF. The data in Fig. 8 indicate that L at a fixed T has a nearly *linear* dependence on ρ rather than the well-known nonanalytical scaling, i.e., $L \sim e^{\Delta h_p/2k_BT}\rho^{1/2}$, predicted by the FA model [13,50,89,90]. This is of physical importance because a near-linear dependence of L on concentration, ρ, has often been reported [91] in wormlike micelles which have also been modeled by the FA equilibrium polymerization model [50]. Clearly, the dipolar interactions are leading to important qualitative effects that are not included in highly simplified models of equilibrium polymerization such as the FA model.

The T dependence of L also deviates substantially from the predictions of the FA model. In Fig. 9, we show the slope $\alpha(T)$ describing the increase in L with ρ. The FA model predicts that L should increase in the classical fashion [13,50], $L(FA) \sim e^{\Delta h_p/2k_BT}$, at a fixed ρ, but the data in Fig. 9 indicate that the exponent is nearly *twice* as large as the FA prediction, as in the case of the concentration scaling exponent. Specifically, the solid line corresponds to the scaling relation $\alpha \sim \exp(E/k_BT)$, where $E=-91.9\varepsilon$ and the dashed line indicates the result of fixing E by the SF intermolecular potential minimum value, $E=\Delta h_p=-100.7\varepsilon$. How can this exponent doubling be understood?

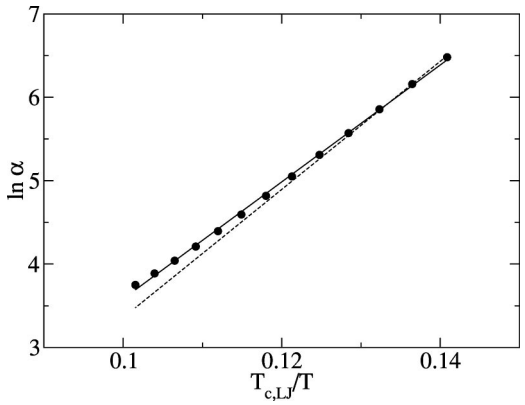

FIG. 9. The parameter α obeys an Arrhenius temperature dependence to a good approximation.

Dudowicz *et al.* [13,83] have noted that a near linear dependence on ρ occurs in equilibrium polymerization models in which the polymerization process occurs subject to *constraints* (e.g., chemical initiation and thermal activation) that create a bottleneck in the polymerization kinetics. Curiously, such kinetic constraints actually lead to a much *sharper* polymerization transition than in equilibrium polymerization in the absence of these constraints (FA model). This comparison is made for a typical experimental value of the initiator concentration, which is quite small so the transition is sharp (nearly a second-order phase transition). Later work showed this same behavior in equilibrium polymerization with a low extent of thermal activation, see Fig. 1b of [13]. Because some unknown "constraints" (branching effects, etc.) may be acting in the SF, we examine the configurational properties of the polymer chains.

C. Radius of gyration as a function of chain mass

Chain branching is an obvious potential source of deviation from the linear chain model in the SF description if this phenomenon becomes prevalent. We thus examine system configurations in the SF at lower T to determine if these structures are apparent. Such structures (rings and "clusters") were anticipated in the original work of De Gennes and Pincus [27], and there have been recent experimental [31–33], simulation [13], and theoretical works [51,57] addressing the nature of this branching process. At present, there are few well-equilibrated data in $d=3$ for which this question can be considered, however.

Figure 10 shows configuration snapshots at $\rho/\rho_{c,LJ}=0.006\,37$ for four different temperatures ($T/T_{c,LJ}=7.56$, 7.10,6.41,5.95). These snapshots are 2D projections of the 3D configurations. A transition from predominately linear chains ($T>T_{\phi}$) to predominately ring polymers ($T<T_p$) evidently occurs upon cooling. This topological transition is a consequence of the system evolving to a state with the lowest energy (rings) [52,92].

Quantitative evidence for this topological transition shows up in the distribution function for the chain radius of gyration, R_g, for the polymers in the transition region ($T/T_{c,LJ}=6.87$, $\rho/\rho_{c,LJ}=0.0102$) where a large number of polymers

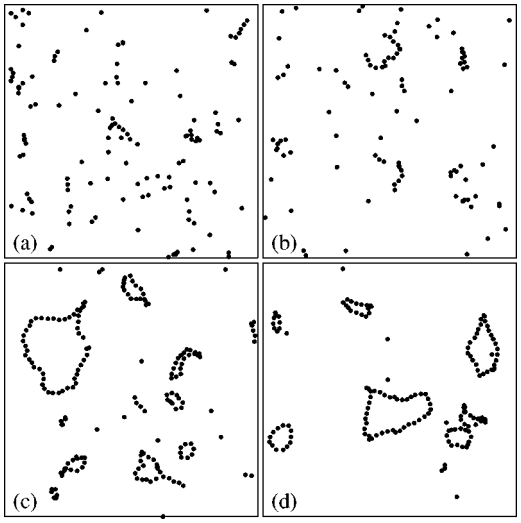

FIG. 10. 2D projection of 3D system configurations for $\rho/\rho_{c,LJ}=0.00637$. (a) $T/T_{c,LJ}=7.56$, (b) $T/T_{c,LJ}=7.10$, (c) $T/T_{c,LJ}=6.41$, (d) $T/T_{c,LJ}=5.95$. At this density, $T_{\Phi}/T_{c,LJ}=7.25$ and $T_p/T_{c,LJ}=7.02$.

and rings coexist. Figure 11 indicates that this distribution function is bimodal with peak position near $R_g^*=0.97$ (rings) and $R_g^*=1.55$ (linear chains) for $N=7$, where $R_g^*=R_g/\sigma$. For simple random walks of rings and linear chains, the ratio of these R_g^* is simply equal to $1/\sqrt{2}\approx 0.71$ while this ratio for SF particles in their ideal (ring and linear chain) minimum energy configuration is 0.54. The observed ratio of 0.63 lies in the middle of these two extremes. We thus infer that the chains and rings can be roughly described as random walks, but with perhaps some swelling due to excluded volume interactions or chain stiffness induced by the deep minimum of the dipolar interaction [27].

We next examine the configurational characteristics of the SF more directly in Fig. 12, where we show R_g^* versus the polymer mass, N. This figure shows R_g^* for a range of N values at a fixed density, $\rho/\rho_{c,LJ}=0.0102$, as open circles and data for all the other densities (leading to better averaging for long chain lengths) as the small dots. A convincing power-law scaling seems to establish itself for $N\geqslant 15$ and a fit of

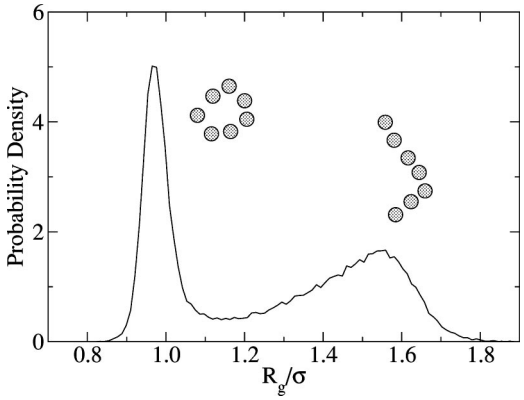

FIG. 11. Radius of gyration probability density for $N=7$ at $T/T_{c,LJ}=6.87$ and $\rho/\rho_{c,LJ}=0.0102$. Representative configurations for a ring and a linear chain are shown.

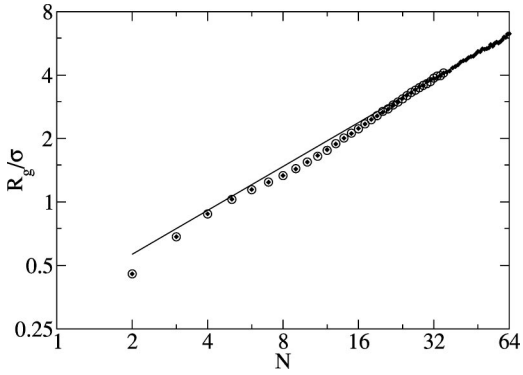

FIG. 12. Radius of gyration versus molecular weight on a log-log plot at $T/T_{c,LJ}=6.85$. The open circles are for $\rho/\rho_{c,LJ}=0.0102$ and the closed symbols are an average across all densities. The slope of the linear fit (solid line) to large N is 0.68. The estimated uncertainties [84] for R_g are less than 1%.

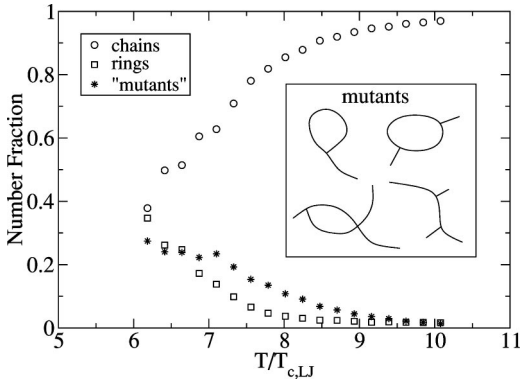

FIG. 13. Number fraction of chains, rings, and other branched structures as a function of temperature at $\rho/\rho_{c,LJ}=0.0191$. The inset shows four examples of the commonly observed mutant structures. These structures represent the chain topologies from actual polymer clusters.

the R_g^* data to a power law ($R_g^* \sim N^\nu$) yields an apparent mass scaling exponent $\nu \approx 0.68 \pm 0.04$. The uncertainty is estimated by considering a range, $10 \leqslant N \leqslant 70$, from which ν can be fit. Our estimate of uncertainty is the range of ν found over this interval. It is notable that this apparent exponent is insensitive to T and ρ and that its value is substantially larger than a self-avoiding walk value, $\nu_{\mathrm{SAW}}=0.59$ [93].

It is likely that the apparent exponent ν is relatively large in comparison to the self-avoiding walk exponent because of semiflexibility effects imparted by the dipolar interaction as mentioned above. This would lead to a slow crossover to the SAW scaling in the long chain asymptotic limit, $N \to \infty$, as seen for uncharged polymers with "bulky beads" [94,95].

There is another possible interpretation of the exponent ν, however. The polymerization transition of rings with directional interactions (consistent with head-to-tail chaining in the SF) is exactly described by the *XY* model [54,96,97] for which the correlation length critical exponent, ν_{xy}, is calculated by RG theory and series analysis to equal $\nu_{xy}=0.67$ in three dimensions [98]. Recent computations have indicated that the R_g exponent ν for the polymers that form in conjunction with the *XY* model phase transition equals the correlation length exponent of this model [99,100], so our finding $\nu=0.68$ is highly suggestive. Further simulations with a larger box size and a larger range of ρ and T are needed to confirm this interesting possible interpretation of the R_g exponent.

The self-organized structures can be divided into three topological categories: chains, rings, and branched structures. A chain is characterized by a cluster which has exactly two particles with one nearest neighbor each and all other particles having exactly two nearest neighbors. A ring is characterized by a cluster in which every particle has exactly two nearest neighbors. A branched structure is neither a chain nor a ring. Two particles are considered neighbors if their separation distance is less than $r_a=1.5\sigma$. In Fig. 13, we observe that the number fraction of chain structures drops precipitously through the polymerization transition, while the number fraction of rings sharply increases upon polymerization. (This effect has been seen experimentally in magnetic nanoparticle fluids [33]. This trend is visually apparent in specific realizations of the fluid as T is lowered (Fig. 10). A feature that is not so clear from the molecular "snapshots" is that there are quite a few clusters that cannot neatly be classified as either rings or chains. De Gennes and Pincus briefly refer to such "cluster" structures [13,27], but we prefer to call these "mutants." Some representative topological representations in two-dimensional projection are shown in the inset of Fig. 13. The number density of these objects actually exceeds those of the rings at higher T in Fig. 13, but at low temperatures below the polymerization transition ($T_\Phi/T_{c,LJ}=8.02$) the number density of the rings exceeds that of the mutants. We note that the concentration of "defect" structures in the model of Tlutsy and Safran [51,57] decreases with decreasing T, rather than increasing upon cooling as in Fig. 13, so that this model is apparently inadequate to describe the topological transition in the SF. The traditional view of ring formation based on the driving force of minimizing the chain energy through the formation of the flux-closure rings [92] apparently provides the correct leading-order description of the origin of the topological transition.

D. Pressure and the theta point

Much of the geometrical complexity of self-organizing systems derives from an interplay between directional interactions and isotropic (van der Waals) interactions. The discussion in previous sections emphasizes the impact of the directional (dipolar) interactions in the SF by taking the ratio of the dipolar to the van der Waals interactions strengths μ^{*2} to be large ($\mu^{*2}=36$), which makes the polymerization transition T higher than the T for phase separation [30]. This choice allowed us to study the polymerization transition in isolation from phase separation. In many systems, these transitions *couple* to create a rich phase separation phenomenology that is quite unlike simple "unassociated" fluids [13]. This situation requires that we determine the isotropic (van der Waals) interactions governing phase separation in addition to the interactions characterizing the directional interactions ($\Delta h_p, \Delta s_p$). In principle, the determination of the interaction parameters governing phase separation should follow

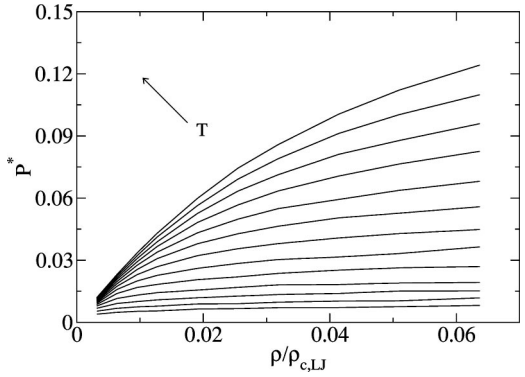

FIG. 14. Dimensionless pressure versus density, $P^*=P\sigma^3/\varepsilon$. The arrow indicates the direction of increasing temperature.

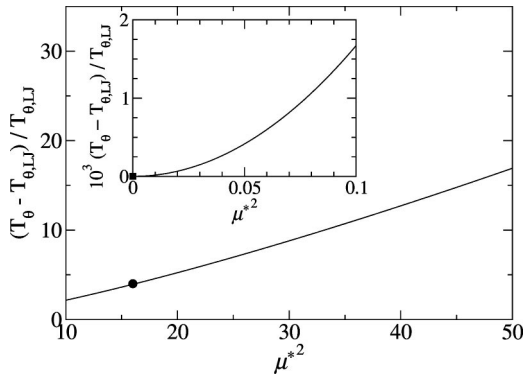

FIG. 16. Exact analytic calculation of $(T_\theta - T_{\theta,LJ})/T_{\theta,LJ}$ versus μ^{*2}. Filled symbols indicate theta point determinations from Fig. 15.

the same procedure as unassociated liquids, but some special problems arise in the associated fluids that require discussion if this task is to be effectively accomplished.

A near constancy of the osmotic pressure as a function of ρ in the absence of phase separation is a commonly observed characteristic of associating fluids generally [101–103], and this phenomenon is naturally expected in the SF. Figure 14 shows the progressive change in P from a linear dependence on ρ for small ρ (ideal gas law) to near independence on ρ as T is lowered from high T through T_Φ. This property of the SF has been noted before [29]. Evidently, the determination of a reliable estimate of the second virial coefficient B_2, our basic measure of the strength of the isotopic van der Waals interaction, could become problematic [36] from a practical standpoint in T ranges in which the pressure P exhibits essentially no dependence on ρ. Note that $P>0$ so that the system is still in the homogeneous (one-phase) region from the standpoint of phase separation.

It is apparent that P does depend on ρ at very low concentrations and we may inquire if these data provide reliable information for the second virial coefficient, B_2. The determination of virial information of this kind is important because we also seek to quantify information regarding the strength of van der Waals interactions responsible for phase separation. The SF is a particularly favorable case for this type of comparison since the second and third virial coefficients [16,20,20] have been determined analytically for this model so that comparison between the exact analytic theory and simulation is possible.

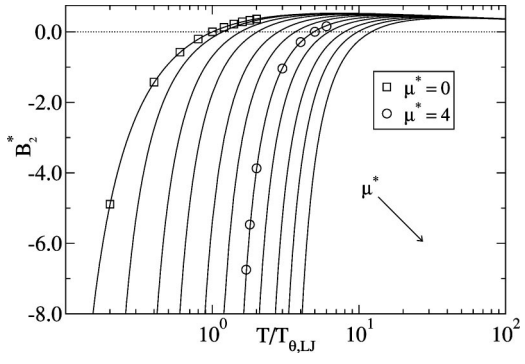

FIG. 15. Second virial coefficient, $B_2^*=B_2/b_0$, versus temperature. $b_0=2\pi N\sigma^3/3$. Lines are from the analytical solution and open symbols are from simulations; squares are for $\mu^*=0$ and circles are for $\mu^*=4$. The arrow indicates the direction of increasing μ^*, $0\leqslant\mu^*\leqslant 6$.

In Fig. 15, we show the exact analytic results for the dimensionless second virial coefficient $B_2^*\equiv 3B_2/(2\pi N\sigma^3)$ of Stockmayer [16] and Rowlinson [20] versus our current simulation (open symbols). Simulation results were calculated by fitting P versus ρ data to the virial equation in the range $0.000\,637\leqslant\rho/\rho_{c,LJ}\leqslant 0.0637$. This comparison shows that it is still possible to determine reliable estimate of B_2 at low concentrations, despite the complications caused by clustering at higher concentrations.

The exact analytic treatment of B_2 allows us to make further statements about other characteristic temperatures of the SF model that are germane to understanding the critical behavior of this model, e.g., the T at which $B_2=0$ ("theta temperature," T_θ, in the polymer literature [93] or the "Boyle temperature" in gas theory [23]). The exact analytic expression for B_2^* is given in the Appendix in the notation of the present paper, and we numerically determined T_θ as a function of μ^{*2} to high accuracy based on this expression. The results of this exercise are shown in Fig. 16. The theta point of the LJ fluid is obtained as the intercept in this figure, $T_{LJ}=3.417\,928\,02(3)\varepsilon/k_B$. The variation of T_θ is roughly linear in μ^{*2} in the case of the critical temperature for phase separation in the SF model [25,30], but this variation is more accurately described by a power law for large $\mu^{*2}(10\leqslant\mu^{*2}\leqslant 50)$,

$$\frac{T_\theta - T_{\theta,LJ}}{T_{\theta,LJ}} = A\mu^{*\alpha}, \tag{17}$$

where $A=0.113$ and $\alpha=2.56$ for which the maximum deviation is 2.5% over the specified μ^* interval. The exponent α apparently has the same limiting value at $\mu^*\to\infty$ as in Eq. (6) for $\varepsilon_{\mu^*}/\varepsilon$, i.e., $\alpha=\frac{8}{3}$. This scaling relation is natural since T_θ is normally proportional to the strength of the intermolecular interaction. The dipolar interaction clearly renormalizes the magnitude of the effective van der Waals interaction so that $T_\theta\sim\varepsilon_{\mu^*}$ for the SF [30]. The dependence of T_θ on μ^{*2}

is nearly quadratic for small values of μ^*. For small μ^{*2} ($0 \leqslant \mu^{*2} < 0.1$), we have the simple approximation

$$\frac{T_\theta - T_{\theta,LJ}}{T_{\theta,LJ}} = B(e^{2\mu^{*4}} - 1), \tag{18}$$

where $B = 0.024\,38$ for which the maximum deviation from the true curve is 0.3% and this variation is shown in the inset to Fig. 16.

Importantly, the magnitude of $T_\theta(\mu^*)$ in the SF is required in the calculation of the phase boundaries of the SF based on a lattice model of equilibrium polymerization [30]. This information is crucial in the analytic modeling because a change in effective value of the van der Waals interaction clearly influences the critical temperature and this renormalization of the van der Waals interaction must be incorporated in any successful theory of the critical behavior of the SF. Previous calculations in Ref. [30] had to rely on much less precise results so that Eqs. (17) and (18) should enable more refined calculations of phase boundaries in the SF.

IV. CONCLUSION

The current interest in the self-organization of particles into polymer chains through weak, but directional, interactions provides an interesting twist in the development of polymer science. Historically, there was a tremendous resistance to the concept that long chain molecules of chemically bound molecular units could exist, and polymers were generally thought of as associating particle systems as we find in the SF [104]. Even until recently, it was normal practice in polymer physics to do everything possible to suppress dynamical clustering processes that could perturb the measurements of the properties of individual chains of invariant chemical structure [105]. The maturation of experimental measurement methods in classical polymer science, and theoretical polymer science generally, provides the necessary tools to make progress in characterizing these hybrid molecular systems involving a combination of chemical and associative polymerization. The exploration of this field is still in its infancy, but promises to be fruitful.

Our simulations indicate that the thermodynamic clustering transition occurring in the SF corresponds to an equilibrium polymerization-type transition. We were able to determine the polymerization transition line by specific heat and order parameter (Φ) determinations and found results semiquantitatively in agreement with the FA model of equilibrium polymerization [13]. An examination of other properties of the SF indicated that the FA model is oversimplified and the model must be generalized to describe the formation of rings and other complex clusters ("mutants") that arise from the dipolar interaction neglected in the analytical modeling.

We also show that clustering in the SF does not make the determination of the second virial coefficient an ill-posed problem in those fluids as we first expected. The results of the exact analytic theory for B_2 agree remarkably with our simulations. We were also able to give exact new results for the theta temperature of the SF for arbitrary reduced dipolar strength μ^*. These exact results are useful for testing MC simulations and as a point of reference in future calculations of the critical properties of the SF.

Future work on the SF should investigate the influence of strong interchain interactions that occur at higher concentrations of SF particles. The simulations of Wei and Patey [42] for essentially the equivalent of the SF fluid [25] indicate the formation of a nematic phase and an associated ferroelectric transition. This ferroelectric transition has been argued to persist even in the liquid state from the presence of long polymers [106]. These simulations seem to imply that the strong interchain interactions at high ρ inhibit the chain-ring transition, leading to the formation of structures (long chains) having large dipole moments. Consistent with this hypothesis, Chen and Dormidontova show that for a donor/acceptor associating system, there is a crossover concentration below which ring formation is favored [58]. It would evidently be interesting to investigate further how the chain-ring topological transition becomes modified at higher ρ in the SF and how these changes reflect themsleves in the dielectric properties of the fluid since this property should be sensitive to the topological form of the clusters.

Real molecules are often characterized by multipolar interactions in addition to dipolar interactions, and we plan to investigate how these multipolar interactions influence supermolecular self-organization. Dijkstra *et al.* [103] have already provided some interesting insights into the structures that form when linear quadrupolar interactions are large, as in the case of exfoliated clay dispersions. They find that *branched* equilibrium polymers form for large quadrupolar interactions rather than the linear chains found for dipolar fluids. Water is characterized by relatively large dipolar and quadrupolar interactions, and the branched transient network structures are known to be responsible for many of the unique properties of this complex fluid [107]. By varying the relative magnitudes of the dipolar and quadrupolar interactions, it should be possible to make a transition between linear and branched equilibrium polymers. The self-organization of sheetlike structures is also a possibility. Apart from these qualitative changes in topological structure, we will concern ourselves with how these additional interactions alter the polymerization transition line position, the geometrical characteristics of the polymers that form, and the nature (e.g., sharpness of transition) of the polymerization transitions that occur in these fluids.

We also plan to consider the influence of monopole (charged) particles on the self-organization of liquids having multipole interactions. The presence of charged particles at the ends of dipolar chains would clearly influence both the propagation of chain growth and the propensity of ring or branched polymer formation. Charged particles could thus play a powerful role in regulating the polymerization process, and investigations of the influence of this coupling between multipolar and charge interactions on self-organization should lead to many interesting effects.

Finally, we note that charged particle fluids such as the restricted primitive model (fluid composed of an equal number of charged spheres of opposite sign and the same diameter) [112] exhibit equilibrium polymerization since the charged particles have a strong propensity to dimerize or to form multipole elements [108,109], which in turn polymerize

as in multipolar fluids. An equilibrium polymerization model has provided an apparently quantitative description of dynamic clustering in a fluid composed of spherical and point-like counterions (a cartoon of polymer solutions) [110], and further studies of equilibrium polymerization in charged fluids provide another fruitful direction in which to extend the present work. Such systems provide a starting point for understanding the ubiquitous dynamic clustering observed in polyelectrolyte solutions [111].

ACKNOWLEDGMENT

KVW would like to thank the NIST NRC Postdoctoral Research Program for financial support.

APPENDIX

The dimensionless second virial coefficient is given by [23]

$$B_2^* = \left(\frac{4}{T^*}\right)^{1/4}\left[\Gamma\left(\frac{3}{4}\right) - \frac{1}{4}\sum_{n=1}^{\infty}\frac{2^n}{n!}\sum_{k=0}^{k\leq n/2}\frac{2^{-3k}}{2k+1}\binom{n}{2k}\Gamma\left(\frac{2n-2k-1}{4}\right)\times\frac{\mu^{*4k}}{T^{*(n+k)/2}}\sum_{m=0}^{k}\frac{\binom{n}{k}3^m}{2m+1}\right], \tag{A1}$$

where $\binom{k}{m}$ etc. denote binomial coefficients. Taking the leading terms in powers of T up to the first term containing μ^*, we have

$$\lim_{T^*\to\infty} B_2^* \sim \left(\frac{4}{T^*}\right)^{1/4}\left\{\Gamma\left(\frac{3}{4}\right) - \frac{1}{2}\Gamma\left(\frac{1}{4}\right)T^{*-1/2} - \frac{1}{2}\Gamma\left(\frac{3}{4}\right)T^{*-1} - \left[\frac{\mu^{*4}}{12}\Gamma\left(\frac{1}{4}\right) + \frac{1}{3}\Gamma\left(\frac{5}{4}\right)\right]T^{*-3/2} + O(T^{*-2})\right\}. \tag{A2}$$

The additive third virial coefficient is not analytically tractable and must be determined by integration from the formal relation [23]

$$C(T^*) = -\frac{1}{4\pi}\int_0^{\infty} r^5 dr \int_0^{1/2} dx \int_0^{[1-(1-x)^2]^{1/2}} y dy \int_0^{\pi} \sin\theta_1 d\theta_1 \times \int_0^{\pi}\sin\theta_2 d\theta_2 \int_0^{\pi}\sin\theta_3 d\theta_3 \int_0^{2\pi} d\phi_1 \int_0^{2\pi} d\phi_2 \times \int_0^{2\pi} d\phi_3 f_{12} f_{13} f_{23}, \tag{A3}$$

where the angles (θ_i, ϕ_i) determine the orientations of the dipoles and where, if r, s, and t are the distances between the centers of the three spheres,

$$s^2 = r^2(x^2 + y^2),$$

$$t^2 = r^2[(1-x)^2 + y^2]. \tag{A4}$$

The functions $f_{ij} = \exp[-u_{ij}/k_B T] - 1$, where u_{ij} is the potential energy between i and j and is given in Eqs. (1) and (2). Rowlinson [20] first evaluated the third virial coefficient but unfortunately introduced an error depending on the dipole moment and temperature [21]. The numerical evaluation of the integrals in Eq. (A3) can be computationally intensive, but progress has been made in improving efficiency by making use of multidimensional nonproduct formulas [22].

[1] D. Philp and J. F. Stoddart, Angew. Chem., Int. Ed. Engl. **35**, 1155 (1996).
[2] J. S. Moore, Curr. Opin. Colloid Interface Sci. **4**, 108 (1999).
[3] J. M. Lehn, *Supramolecular Chemistry* (VCH, Weinheim, 1995).
[4] A. P. Alivisatos, K. P. Johnsson, X. G. Peng, T. E. Wilson, C. J. Loweth, M. P. Bruchez, and P. G. Schultz, Nature (London) **382**, 609 (1996).
[5] J. H. K. K. Hirschberg, L. Brunsveld, A. Ramzi, J. A. J. M. Vekemans, R. P. Sijbesma, and E. W. Meijer, Nature (London) **407**, 167 (2000).
[6] C. E. Flynn, S. W. Lee, B. R. Peele, and A. M. Belcher, Acta Mater. **51**, 5867 (2003).
[7] B. J. de Gans, S. Wiegand, E. R. Zubarev, and S. I. Stupp, J. Phys. Chem. B **106**, 9730 (2002); S. I. Stupp, S. Son, H. C. Lin, and L. S. Li, Science **259**, 59 (1993); S. I. Stupp, V. LeBonheur, K. Walker, L. S. Li, K. E. Huggins, M. Keser, and A. Amstutz, *ibid.* **276**, 384 (1997).
[8] C. A. Mirkin, R. L. Letsinger, R. C. Mucic, and J. J. Storhoff, Nature (London) **382**, 607 (1996).
[9] R. P. Sijbesma, F. H. Beijer, L. Brunsveld, B. J. B. Folmer, J. H. K. K. Hirschberg, R. F. M. Lange, J. K. L. Lowe, and E. W. Meijer, Science **278**, 1601 (1997).
[10] A. K. Boal, F. Ilhan, J. E. DeRouchey, T. Thurn-Albrecht, T. P. Russell, and V. M. Rotello, Nature (London) **404**, 746 (2000).
[11] J. Dudowicz, K. F. Freed, and J. F. Douglas, J. Chem. Phys. **113**, 434 (2000).
[12] J. Dudowicz, K. F. Freed, and J. F. Douglas, J. Chem. Phys. **112**, 1002 (2000).
[13] J. Dudowicz, K. F. Freed, and J. F. Douglas, J. Chem. Phys. **119**, 12 645 (2003).
[14] J. T. Kindt and W. M. Gelbart, J. Chem. Phys. **114**, 1432 (2001).
[15] J. Herzfeld, Acc. Chem. Res. **29**, 31 (1996).
[16] W. H. Stockmayer, J. Chem. Phys. **9**, 383 (1941).
[17] P. Terech and R. G. Weiss, Chem. Rev. (Washington, D.C.) **97**, 3133 (1997).
[18] P. Terech, C. Rossat, and F. Volino, J. Colloid Interface Sci. **227**, 363 (2000).
[19] P. Terech, Ber. Bunsenges. Phys. Chem. **102**, 1630 (1998).

[20] J. S. Rowlinson, Trans. Faraday Soc. **45**, 974 (1949); J. Chem. Phys. **19**, 827 (1951); **19**, 831 (1951).
[21] D. E. Stogryn, J. Chem. Phys. **50**, 4967 (1969).
[22] C. H. J. Johnson and T. H. Spurling, Aust. J. Chem. **24**, 1567 (1971).
[23] J. O. Hirschfelder, C. F. Curtiss, and R. B. Bird, *Molecular Theory of Gases and Liquids* (John Wiley, New York, 1954).
[24] M. E. vanLeeuwen and B. Smit, Phys. Rev. Lett. **71**, 3991 (1993).
[25] M. J. Stevens and G. S. Grest, Phys. Rev. E **51**, 5962 (1995).
[26] P. C. Jordan, Mol. Phys. **25**, 961 (1973).
[27] P. G. de Gennes and P. A. Pincus, Phys. Kondens. Mater. **11**, 189 (1970).
[28] J. M. Tavares, M. M. TelodaGama, and M. A. Osipov, Phys. Rev. E **56**, R6252 (1997).
[29] P. I. C. Teixeira, J. M. Tavares, and M. M. T. da Gama, J. Phys.: Condens. Matter **12**, R411 (2000).
[30] J. Dudowicz, K. F. Freed, and J. F. Douglas, Phys. Rev. Lett. **92**, 045502 (2004).
[31] A. P. Philipse and D. Maas, Langmuir **18**, 9977 (2002).
[32] K. Butter, P. H. H. Bomans, P. M. Frederik, G. J. Vroege, and A. P. Philipse, Nat. Mater. **2**, 88 (2003).
[33] V. F. Puntes, K. M. Krishnan, and A. P. Alivisatos, Science **291**, 2115 (2001).
[34] D. J. Pochan, J. P. Schneider, J. Kretsinger, B. Ozbas, K. Rajagopal, and L. Haines, J. Am. Chem. Soc. **125**, 11 802 (2003).
[35] B. Tripišová and J. A. Brown, Int. J. Mod. Phys. B **12**, 543 (1998).
[36] J. O. Hirschfelder, F. T. McClure, and I. F. Weeks, J. Chem. Phys. **10**, 201 (1942).
[37] J. D. Lambert, G. A. H. Roberts, J. S. Rowlinson, and V. J. Wilkinson, Proc. R. Soc. London, Ser. A **196**, 8 (1949).
[38] E. A. Alexander and J. D. Lambert, Trans. Faraday Soc. **37**, 421 (1941).
[39] K. Pitzer, J. Am. Chem. Soc. **77**, 3427 (1955).
[40] R. E. Rosensweig, *Ferrohydrodynamics* (Cambridge University Press, Cambridge, 1985).
[41] *Magnetic Fluids and Applications Handbook*, edited by B. Berkovski and V. Bashtovoy (Begell House, Inc., New York, 1996).
[42] D. Wei and G. N. Patey, Phys. Rev. Lett. **68**, 2043 (1992).
[43] J. C. Shelley and G. N. Patey, J. Chem. Phys. **103**, 8299 (1995).
[44] J. M. Romero-Enrique, L. F. Rull, and A. Z. Panagiotopoulos, Phys. Rev. E **66**, 041204 (2002).
[45] S. C. McGrother and G. Jackson, Phys. Rev. Lett. **76**, 4183 (1996).
[46] R. vanRoij, Phys. Rev. Lett. **76**, 3348 (1996).
[47] R. P. Sear, Phys. Rev. Lett. **76**, 2310 (1996).
[48] M. A. Osipov, P. I. C. Teixeira, and M. M. TelodaGama, Phys. Rev. E **54**, 2597 (1996).
[49] J. M. Tavares, J. J. Weis, and M. M. TelodaGama, Phys. Rev. E **65**, 061201 (2002).
[50] M. E. Cates and S. J. Candau, J. Phys.: Condens. Matter **2**, 6869 (1990).
[51] T. Tlusty and S. A. Safran, Science **290**, 1328 (2000).
[52] H. B. Lavender, K. A. Iyer, and S. J. Singer, J. Chem. Phys. **101**, 7856 (1994).
[53] T. Banks, R. Myerson, and J. Kogut, Nucl. Phys. B **129**, 493 (1977).
[54] C. Dasgupta and B. I. Halperin, Phys. Rev. Lett. **47**, 1556 (1981).
[55] J. Toner, Phys. Rev. B **26**, R462 (1982).
[56] A. Z. Panagiotopoulos, J. Chem. Phys. **109**, 10 914 (1998).
[57] J. T. Kindt, J. Phys. Chem. B **106**, 8223 (2002).
[58] C. C. Chen and E. E. Dormidontova, Macromolecules **37**, 3905 (2004).
[59] J. C. Shelley, G. N. Patey, D. Levesque, and J. J. Weis, Phys. Rev. E **59**, 3065 (1999).
[60] B. Chen and J. I. Siepmann, J. Phys. Chem. B **105**, 11 275 (2001).
[61] U. H. E. Hansmann, Chem. Phys. Lett. **281**, 140 (1997).
[62] M. G. Wu and M. W. Deem, Mol. Phys. **97**, 559 (1999).
[63] F. Wang and D. P. Landau, Phys. Rev. Lett. **86**, 2050 (2001).
[64] R. Faller and J. J. de Pablo, J. Chem. Phys. **119**, 4405 (2003).
[65] T. Liu, V. M. Nace, and B. Chu, Langmuir **15**, 3109 (1999).
[66] Z. K. Zhou, B. Chu, and V. M. Nace, Langmuir **12**, 5016 (1996).
[67] M. A. Floriano, E. Caponetti, and A. Z. Panagiotopoulos, Langmuir **15**, 3143 (1999).
[68] J. W. Zhuang, A. P. Andrews, and S. C. Greer, J. Chem. Phys. **107**, 4705 (1997).
[69] P. S. Niranjan, P. B. Yim, J. G. Forbes, S. C. Greer, J. Dudowicz, K. F. Freed, and J. F. Douglas, J. Chem. Phys. **119**, 4070 (2003).
[70] A. G. Kalampounias, K. S. Andrikopoulos, and S. N. Yannopoulos, J. Chem. Phys. **118**, 8460 (2003).
[71] F. W. Starr, J. F. Douglas, and S. C. Glotzer, J. Chem. Phys. **119**, 1777 (2003).
[72] J. E. Eldridge and J. D. Ferry, J. Phys. Chem. **58**, 992 (1954).
[73] H. M. Tan, A. Moet, A. Hiltner, and E. Baer, Macromolecules **16**, 28 (1983).
[74] S. Mal, P. Maiti, and A. K. Nandi, Macromolecules **28**, 2371 (1995).
[75] A. Coniglio, H. E. Stanley, and W. Klein, Phys. Rev. Lett. **42**, 518 (1979).
[76] F. Tanaka and A. Matsuyama, Phys. Rev. Lett. **62**, 2759 (1989).
[77] S. K. Kumar and J. F. Douglas, Phys. Rev. Lett. **87**, 188301 (2001).
[78] M. C. Grant and W. B. Russel, Phys. Rev. E **47**, 2606 (1993).
[79] C. J. Rueb and C. F. Zukoski, J. Rheol. **41**, 197 (1997).
[80] H. Verduin and J. K. G. Dhont, J. Colloid Interface Sci. **172**, 425 (1995).
[81] S. C. Greer, J. Phys. Chem. B **102**, 5413 (1998).
[82] S. C. Greer, Adv. Chem. Phys. **94**, 261 (1996).
[83] J. Dudowicz, K. F. Freed, and J. F. Douglas, J. Chem. Phys. **111**, 7116 (1999).
[84] The estimated uncertainty is referred to as the "estimated error" and denoted by σ in M. P. Allen and D. J. Tildesley, *Computer Simulation of Liquids* (Oxford University Press, New York, 1989), Chap. 6.4.1.
[85] F. S. Dainton and K. J. Ivin, Nature (London) **162**, 705 (1948).
[86] J. Dudowicz, K. F. Freed, and J. F. Douglas (unpublished results).
[87] I. G. Economou and M. D. Donohue, AIChE J. **37**, 1875 (1991).
[88] M. S. Wertheim, J. Stat. Phys. **35**, 35 (1984); **42**, 459 (1986); **42**, 477 (1986); J. Chem. Phys. **87**, 7323 (1987).
[89] A. Milchev and D. P. Landau, Phys. Rev. E **52**, 6431 (1995).

[90] J. P. Wittmer, A. Milchev, and M. E. Cates, J. Chem. Phys. **109**, 834 (1998).
[91] P. Schurtenberger, C. Cavaco, F. Tiberg, and O. Regev, Langmuir **12**, 2894 (1996).
[92] I. S. Jacobs and C. P. Bean, *Magnetism* (Academic Press, New York, 1963), Vol. 3.
[93] K. F. Freed, *Renormalization Group Theory of Macromolecules* (J. Wiley, New York, 1987).
[94] M. Bishop and J. P. J. Michels, J. Chem. Phys. **84**, 444 (1986).
[95] D. E. Kranbuehl and P. H. Verdier, Macromolecules **25**, 2557 (1992).
[96] G. Kohring, R. E. Shrock, and P. Wills, Phys. Rev. Lett. **57**, 1358 (1986).
[97] J. H. Akao, Phys. Rev. E **53**, 6048 (1996).
[98] R. Guida and J. Zinn-Justin, J. Phys. A **31**, 8103 (1998).
[99] N. K. Kultanov and Y. Lozovik, Phys. Lett. A **223**, 189 (1996).
[100] J. Kiskis, R. Narayanan, and P. Vranas, J. Stat. Phys. **73**, 765 (1993).
[101] H. Wennerstrom and B. Lindman, Phys. Rep. **52**, 1 (1979).
[102] A. Mourchid, A. Delville, J. Lambard, E. Lecolier, and P. Levitz, Langmuir **11**, 1942 (1995).
[103] M. Dijkstra, J. P. Hansen, and P. A. Madden, Phys. Rev. Lett. **75**, 2236 (1995).
[104] H. Morawetz, Angew. Chem., Int. Ed. Engl. **26**, 93 (1987).
[105] W. Burchard, P. Lang, L. Schulz, and T. Coviello, Makromol. Chem., Macromol. Symp. **58**, 21 (1992).
[106] S. Klapp and F. Forstmann, Phys. Rev. E **60**, 3183 (1999).
[107] R. M. LyndenBell and J. C. Rasaiah, J. Chem. Phys. **107**, 1981 (1997).
[108] Q. L. Yan and J. J. de Pablo, Phys. Rev. Lett. **88**, 095504 (2002).
[109] J. M. Romero-Enrique, G. Orkoulas, A. Z. Panagiotopoulos, and M. E. Fisher, Phys. Rev. Lett. **85**, 4558 (2000).
[110] S. Bastea, Phys. Rev. E **66**, 020801 (R) (2002).
[111] Y. Zhang, J. F. Douglas, B. D. Ermi, and E. J. Amis, J. Chem. Phys. **114**, 3299 (2001).
[112] The interaction energy of the RPM is normally defined in terms of the energy of a positively (ze) and negatively ($-ze$) charged spherical ion of radius σ in contact. This configuration of charges defines a dipole of moment $\mu=ze\sigma$, thus defining a relationship between the interaction parameters governing monopole (RPM) and dipolar fluids.